Research Square

Preprints are preliminary reports that have not undergone peer review.
They should not be considered conclusive, used to inform clinical practice,
or referenced by the media as validated information.

An Experimental Study on the Tractive Performance of a Single Tire according to Normal Load in Sandy Soil

Se-O Choi
Pusan National University
Min-Seung Kim
Pusan National University
Dae-Wi Jung
Pusan National University
Shin-Young Noh
Pusan National University
Ye-Na Lee
Pusan National University
Yeon-Soo Kim
yskim23@pusan.ac.kr
Pusan National University
Yong-Joo Kim
Chungnam National University

Research Article

Keywords: Soil-Tire interaction, Normal load, Tractive performance, Single tire

Posted Date: March 9th, 2026

DOI: https://doi.org/10.21203/rs.3.rs-8842654/v1

License: This work is licensed under a Creative Commons Attribution 4.0 International License.
Read Full License

Additional Declarations: No competing interests reported.

Version of Record: A version of this preprint was published at Journal of Biosystems Engineering on August 24th, 2026. See the published version at https://doi.org/10.1007/s42853-026-00305-3.

<< Manuscript >>

General guideline

Text formatting

- Manuscript should be submitted in MS Word.
- Use a normal, plain font (suggestion: Times New Roman, 12-point) for text.
- Set double line spacing with line numbers on the left margin.
- Use italics for emphasis.
- Use the automatic page numbering function to number the pages.
- Do NOT use field functions.
- Use tab stops or other commands for indent, not the space bar.
- Use the table function, not spreadsheets to make tables.
- Use the equation editor or MathType for equations.
- Save your file in docx format (Word 2007 or higher) or doc format (older Word versions).

Headings

- Please use no more than three levels of displayed headings.

Footnotes

- Footnotes can be used to give additional information, which may include the citation of a reference included in the reference list. They should not consist solely of a reference citation, and they should never include the bibliographic details of a reference. They should also not contain any figures or tables.
- Footnotes to the text are numbered consecutively; those to tables should be indicated by superscript lower-case letters (or asterisks for significance values and other statistical data). Footnotes to the title or the authors of the article are not given reference symbols.
- Always use footnotes instead of endnotes.

An Experimental Study on the Tractive Performance of a Single Tire according to Normal Load in Sandy Soil

Abstract

Purpose The purpose of this study was to experimentally investigate the effects of normal load variation on the tractive performance of a single tire under sandy soil conditions using an indoor soil-bin test system.

Methods Straight-line traveling tests were conducted at a constant theoretical traveling speed of 0.5 m/s while varying the applied normal load at five levels (0, 10, 20, 30, and 40 kg). Dry sandy soil with a particle size of 0.18-0.20 mm and negligible water content was used to ensure experimental repeatability. For each load condition, the tire traveled 3 m, and each test was repeated five times. Soil thrust was estimated from the driving motor torque, slip ratio was calculated from the difference between theoretical and actual traveling distances, and slip efficiency was derived from the slip ratio. In addition, a gross traction coefficient was introduced as a normalized index by dividing soil thrust by the vertical dynamic load.

Results The average soil thrust increased from 27.07 N at 0 kg to 47.19 N at 40 kg, corresponding to a 1.74-fold increase, indicating that normal load strongly influences soil thrust generation under sandy soil conditions. In contrast, slip ratio and slip efficiency exhibited non-monotonic behavior, with the minimum slip ratio (46.90%) and maximum slip efficiency (53.10%) occurring at the 20 kg condition. The gross traction coefficient ranged from approximately 0.04 to 0.05 and also showed non-monotonic variation with increasing normal load.

Conclusions The results demonstrate that increasing normal load enhances the absolute magnitude of soil thrust but does not necessarily improve tractive performance due to increased slip under high-load conditions. An optimal normal load condition exists in sandy soil that cannot be identified based on soil thrust magnitude alone. The soil-bin-based experimental results provide reliable benchmark data for understanding soil-tire interaction and for validating numerical soil-tire interaction models.

Keywords: Soil-Tire interaction, Normal load, Tractive performance, Single tire

Introduction

Major industrial off-road vehicles, such as agricultural and construction machinery, primarily operate on deformable terrains including soft ground, tilled soil, and unpaved surfaces rather than paved roads. These ground conditions have a direct influence on vehicle tractive performance and driving stability. In particular, experiments conducted under agricultural field conditions often suffer from reduced data reliability due to spatial variability

of soil properties and abrupt environmental changes (Roozbahani et al., 2013). Therefore, a quantitative understanding of soil-tire interaction characteristics is essential for improving the mobility and traction performance of off-road vehicles.

Tire performance is governed by multiple interacting factors, which limits the ability to evaluate the effect of each factor independently. Among these factors, the vertical load applied to the tire directly affects the contact area and sinkage depth, which are closely related to soil shear resistance and thrust generation mechanisms (Alkhalifa et al., 2024). Recent studies have reported that variations in vertical load significantly alter soil-tire contact conditions and act as a key parameter influencing traction force, slip ratio, and energy loss characteristics (Farhadi et al., 2020). Moreover, soil is a highly nonlinear material whose mechanical behavior and physical properties vary considerably depending on environmental factors such as particle size distribution, water content, compaction state, and interparticle bonding. As a result, even under identical tire and loading conditions, slip behavior and soil thrust may vary substantially according to soil state (Jjagwe et al., 2023). Consequently, a clear understanding of soil-tire interaction characteristics under varying vertical load conditions is a critical factor in evaluating off-road vehicle performance and establishing design criteria.

Studies on soil-tire interaction have traditionally been conducted based on terramechanics theory. Previous research has attempted to explain thrust generation mechanisms by considering soil shear strength characteristics, soil-tire contact conditions, and vertical loading, and has sought to quantify machine performance indicators such as slip ratio and thrust, as well as internal soil stress and shear behavior (Bailey et al., 1996; Calleja-Huerta et al., 2023). Tiwari et al., (2010) employed analytical and empirical approaches to predict the traction performance of a single tire and developed soil-specific traction models. Mardani & Golanbari,

(2024) experimentally investigated soil-tire interaction by operating a traction device under controlled soil conditions and measuring soil reaction forces and traction force, thereby quantitatively evaluating traction characteristics according to soil conditions. Gee-Clough, (1976) analyzed rolling resistance and sinkage behavior of rigid wheels by comparing experimental results with predictions based on the Bekker theory, demonstrating that rolling resistance and sinkage characteristics vary with ground condition and sinkage level. Zeng et al., (2022) experimentally evaluated the tractive performance of agricultural tires on granular soil using a single-wheel test apparatus, showing that tire load and slip conditions significantly affect traction force and traction coefficient.

Although these studies have provided a theoretical foundation for predicting vehicle mobility, optimizing tire design, and improving operating conditions for agricultural machinery, full-scale field experiments often exhibit limited reproducibility and quantitative reliability due to soil heterogeneity, environmental variability, and difficulties in repeated testing (Ptak et al., 2023).

As an alternative approach to overcome these limitations, experimental studies utilizing soil-bin test facilities have been widely adopted (Kawase et al., 2006). Soil-bin test systems enable artificial preparation of soil conditions and precise control of vertical load and traveling speed, making them particularly suitable for isolating the effects of specific variables (Mahadi et al., 2017). In addition, repeated experiments under identical conditions improve experimental reliability and allow stable measurement of key mobility indicators such as soil thrust, slip ratio, and contact characteristics (Kawase et al. 2006). For these reasons, soil-bin test facilities have become a core experimental platform in terramechanics-based research (Bahrami et al., 2023; Tag(Bahrami et al., 2023; Taghavifar et al., 2014; Taghavifar & Mardani, 2014).

Previous soil-bin-based studies have mainly focused on thrust characteristics as a function of slip ratio, differences in traction performance according to tire geometry or tread pattern, or variations in mobility performance depending on soil type (Ani et al., 2018). Although some studies have reported the influence of vertical load on tire contact characteristics and thrust generation (Shmulevich et al., 1996; Zoz & Grisso, 2003), systematic investigations that simultaneously compare slip ratio, soil thrust, and slip efficiency under varying vertical load conditions on the same soil are relatively limited.

Recently, numerical approaches such as the discrete element method (DEM) and multi-body dynamics (MBD) have been increasingly employed to simulate soil-tire interaction (Karpman et al., 2020). While these methods offer the advantage of analyzing microscale behaviors that are difficult to capture experimentally (Yang et al., 2020), experimental validation data are essential to ensure the reliability of simulation results (Zhou et al., 2021). In particular, experimental data describing soil thrust and slip behavior under varying vertical load conditions are critical for calibrating numerical models, yet such datasets remain insufficient.

Soil-bin-based experimental studies can therefore play a key role in the initial calibration and validation of numerical soil-tire interaction models (Bahrami et al., 2023). Accordingly, the objective of this study is to quantitatively analyze the effects of vertical load variation on tire tractive performance and slip efficiency under constant straight-line traveling conditions using a soil-bin. Dry sandy soil, which exhibits relatively simple particle morphology and high experimental repeatability, was selected as the test medium. To compensate for the limitations of the test system, in which rolling resistance and traction force cannot be directly measured, an additional performance indicator—the gross traction coefficient—was introduced by normalizing the total soil thrust generated at the soil-tire interface by the vertical dynamic load.

The torque and rotational speed measured at the driving motor represent the input load applied to the system and are closely associated with soil deformation and slip behavior during travel. In sandy soil, variations in vertical load alter soil shear resistance characteristics; therefore, even under identical traveling speed conditions, the required driving torque and slip behavior may differ. In this study, slip efficiency defined based on slip ratio is employed to evaluate how effectively the input load contributes to actual vehicle motion as vertical load increases.

While previous soil-bin studies mainly examined thrust-slip relationships or traction force independently, limited attention has been given to the combined evaluation of soil thrust, slip ratio, slip efficiency, and a normalized gross traction coefficient under identical soil and traveling conditions. Accordingly, the present study provides a systematic comparison of these performance indicators while varying only the vertical load, thereby distinguishing between the absolute mobilization of soil shear resistance and the efficiency of converting input load into actual motion. The results reveal non-monotonic slip-related responses with increasing vertical load and demonstrate the existence of an optimal load condition in dry sandy soil. Furthermore, the controlled soil-bin dataset obtained in this study offers reliable benchmark data for the calibration and validation of numerical soil-tire interaction models, including DEM-MBD coupled simulations.

Materials and Methods

Soil-bin Test System Configuration

Specifications of the Soil-bin

Tire tractive performance tests were conducted using a soil-bin configured as shown in Fig.

129 1.

130



131

132 **Fig. 1** Schematic of the soil-bin: drive unit (A), pulley and belt (B), DAQ system (C), soil

133 (sand, D), and LM guide (E).

134

135 The soil-bin test facility had overall dimensions of 6 × 2 × 1 m (length × width × height).

136 Linear motion (LM) guides were installed on both sides of the drive unit to enable forward and

137 backward motion. The drive unit had dimensions of 335 × 370 × 415 mm (width × depth ×

138 height), and a vertical loading rod connected to a circular plate was installed to apply various

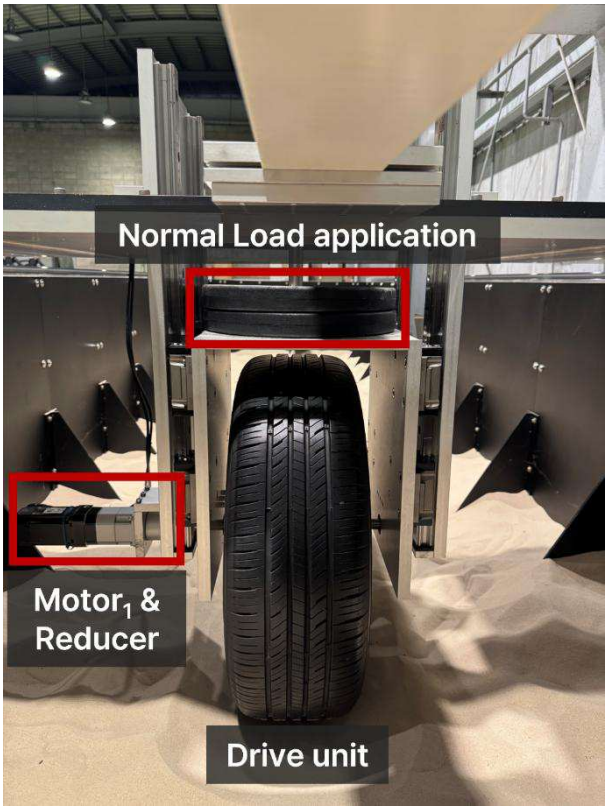
139 levels of vertical load to the tire.

140 In addition, LM guides were installed between the drive unit and the fixed frame, allowing

141 vertical movement of the drive unit when vertical loads were applied or when surface

142 irregularities were present. This configuration enabled vertical displacement of the drive unit
143 while maintaining straight-line motion during testing. The configuration of the drive unit under
144 applied vertical load conditions during the soil-bin test is shown in Fig. 2.

145



146

147 **Fig. 2** Drive unit of the soil-bin.

148

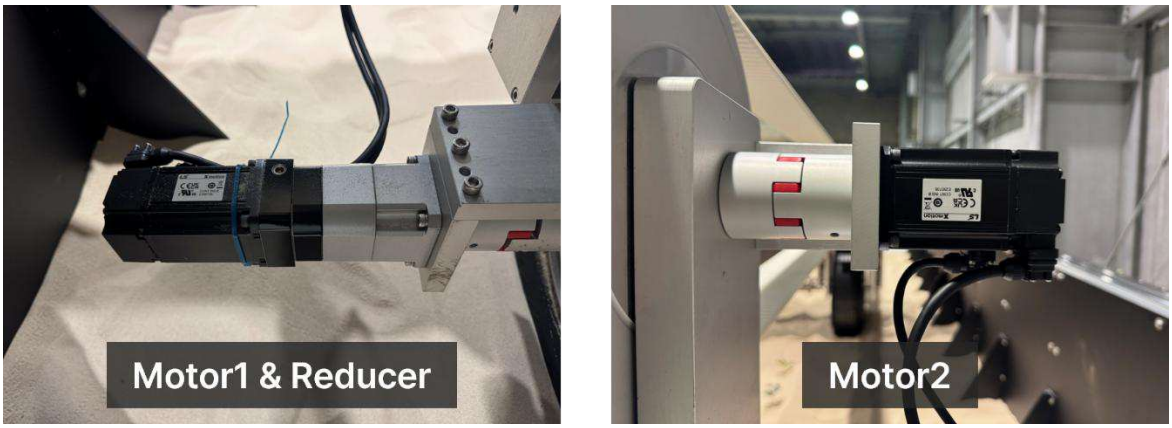
149 **Tire Drive System**

150 To drive the tire, a first motor (Motor1) and a reducer were coupled to the tire axle. A second
151 motor (Motor2), without a reducer, was mounted on the pulley used to drive the belt connected
152 to the drive unit. Servo motors (APMC-FBL04AMK, LS Electric, Anyang, Republic of Korea)
153 were used, and a reducer with a reduction ratio of 50 (PGX62-H-50, ATG, Taiwan) was

154 employed.

155 Based on the performance characteristics of the motor and reducer, the tire was capable of
156 operating at a maximum rotational speed of 3000 rpm. Photographs of the motors and reducer
157 are shown in Fig. 3, and the detailed specifications of the servo motor and reducer are
158 summarized in Table 1 and Table 2, respectively.

159



160

161 **Fig. 3** Servo motors and reducer.

162

163 **Table 1** Specifications of the servo motor

Unit	Value
Rate power (kW)	0.4
Rate torque (N·m)	1.27
Peak torque (N·m)	3.82
Rated current (A)	2.6

Maximum current (A)	7.8
Rated speed (rpm)	3000
Maximum speed (rpm)	5000

Table 2 Specifications of the reducer

Unit	Value
Reduction ratio	50
Rated output torque (N·m)	45
Maximum output torque (N·m)	Tree times the rated output torque (135)
Rated input speed (rpm)	3000
Maximum input speed (rpm)	6000
Maximum axial load (N)	560
Maximum radial load (N)	1120

Soil Selection for the Soil-bin Test

The soil used in this study was selected as dry sandy soil with a particle size range of 0.18-0.20 mm. Compared with actual agricultural field soil, this soil exhibits relatively simple particle morphology and low heterogeneity, making it suitable for initial calibration of numerical simulations and ensuring high experimental repeatability.

Selection of the Test Tire

The test tire used in this study was a passenger car tire (Smart Plus 2, Hankook Tire, Seongnam, Republic of Korea) with a size of 205/60R16, as shown in Fig. 4. The mass of the tire was 19.15 kg, and the total mass of the drive unit including the mounted tire was 63.05 kg.



Fig. 4 Specifications and dimensions of the test tire.

Because the sandy soil used in the soil-bin test exhibited low cohesion, soil thrust generated during soil-tire interaction was primarily governed by the applied vertical load rather than the contact area. Therefore, instead of using an agricultural tire with lugs and a large contact area, a general passenger car tire was selected to quantitatively analyze the effect of vertical load variation on soil thrust under sandy soil conditions.

A passenger car tire was intentionally selected to isolate the fundamental effects of vertical load on soil-tire interaction under controlled soil-bin conditions. Unlike agricultural lug tires, which introduce additional complexities associated with lug penetration, soil bulldozing, and

tread-induced disturbances (Koolen & Kuipers, 1983; Wong, 2024), the selected tire provides a relatively smooth contact interface, allowing the influence of vertical load on soil shear mobilization and slip behavior to be examined with minimal geometric interference.

It should be noted that the objective of this study is not to reproduce the absolute tractive performance of agricultural or construction machinery, but rather to investigate fundamental load-dependent soil-tire interaction mechanisms. Accordingly, the results of this study should be interpreted as benchmark data obtained under controlled experimental conditions, rather than as direct predictors of field-scale tractive performance for lugged tires.

Soil Property Measurement

Measurement of Physical Soil Properties

soil thrust and slip ratio vary depending on the physical and mechanical properties of the soil. Therefore, in this study, the fundamental physical properties of the soil used in the soil-bin were measured prior to the experiments to ensure the reproducibility and interpretability of the experimental results. These soil properties were used as baseline data to quantitatively define the test conditions for the tire traveling experiments conducted in this study.

Soil texture was determined according to the soil classification system of the United States Department of Agriculture (USDA) using a sieve shaker (HJ-2153, Heungjin, Gimpo, Republic of Korea).

The measurement of soil physical properties was conducted following the grid sampling method described by Tan (2005). The soil-bin area was divided into 16 grids with dimensions of 0.75 m × 0.75 m. Soil samples were collected using a 100 mL stainless steel cylinder (DIK-

211 1801, Daiki Rika Co., Akagidai, Japan) and a soil sampling device (DIK-1815, Daiki Rika
212 Kogyo Co., Ltd., Akagidai, Japan), as illustrated in Fig. 5.

213



214

215 **Fig. 5** Soil sampling procedure in soil-bin experiment.

216 Two soil samples were collected from each grid, resulting in a total of 32 samples. The mass
217 of each soil sample was measured. The bulk density of each sample was calculated using Eq.
218 1, and the average bulk density was obtained.

219 $$\rho_b = \frac{m_s}{V} \qquad (1)$$

220 Where ρ_b: Bulk density, m_s: Mass of the soil sample, V: Volume of the stainless steel
221 cylinder.

222

223 In addition, the water content of each sample was a calculated using Eq. 2, and the average
224 value was determined.

$$\mathrm{W}\ (\%) = \frac{W_W}{W_S} \times 100 \qquad (2)$$

Where W: Water content, W_S: Weight of the solid fraction, W_W: Weight of the liquid fraction.

Measurement of Mechanical Soil Properties

Traction-related performance parameters, such as soil thrust and slip ratio generated during tire travel, are influenced by the mechanical properties of the soil (Kim et al., 2020). To evaluate the shear strength characteristics of the soil, a direct shear test was conducted. Among the mechanical soil properties, cohesion (c) and internal friction angle ($\emptyset$) were measured in accordance with the KS F 2343 standard test method. The shear strength parameters obtained from the direct shear test were used as fundamental data for quantitatively comparing soil shear resistance characteristics and for analyzing tractive performance (Park & Jeong, 2018).

Soil-bin Test Procedure

Experimental Design

An overview of the experimental procedure for the soil-bin test conducted in this study is shown in Fig. 6.

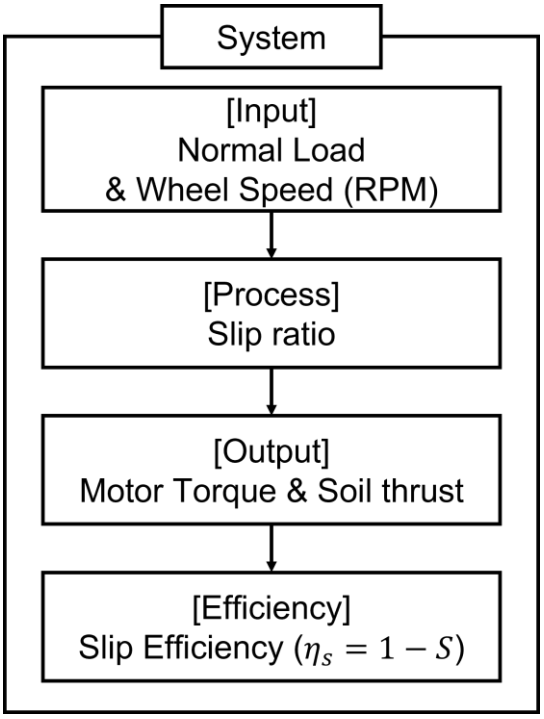


Fig. 6 Schematic overview of the experimental procedure for the soil-bin test.

The experiments were performed by setting the vertical load and wheel rotational speed as input conditions and inducing soil-tire interaction during straight-line travel at a constant speed. During the traveling process, slip may occur due to soil-tire interaction. The slip ratio was calculated using the difference between the theoretical traveling distance of the tire and the actual traveling distance. As an output parameter, variations in the driving motor torque were measured.

Subsequently, soil thrust was estimated based on the measured motor torque in order to quantitatively evaluate how the load input to the tire drive system was converted into effective propulsive force at the ground. Finally, slip efficiency was calculated using the slip ratio to quantitatively assess how efficiently the input load to the tire drive system was converted into actual traveling performance under varying vertical load conditions.

To analyze the characteristics of soil thrust and slip ratio according to changes in vertical load, as well as to evaluate the load demand on the driving motor, straight-line traveling tests were conducted using the soil-bin. The tests were designed to maintain identical traveling conditions under different vertical load levels. In addition, to ensure data reliability under varying vertical load conditions, the soil surface condition and height were maintained uniformly. As shown in Fig. 7, the soil surface was leveled using a roller, and the leveling process was performed before each repeated test.

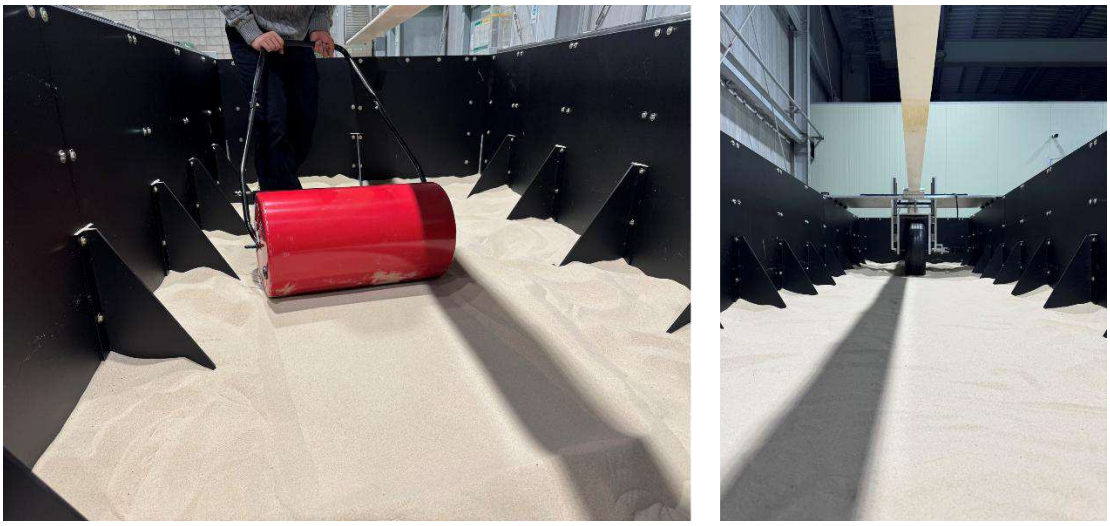


Fig.7 Soil surface leveling process prior to testing.

The vertical load was set to five levels: 0, 10, 20, 30, and 40 kg, considering the performance limits of the motor. In sandy soil, vertical load has a greater influence on soil thrust than contact area; therefore, vertical load was selected as the primary experimental variable. The same test procedure was applied under each vertical load condition, and the tire was controlled to move in a straight line at a constant traveling speed during the test.

The traveling speed was fixed at 0.5 m/s, and the traveling distance for each test was set to 3 m. By applying identical traveling speed and distance under all vertical load conditions, the effects of vertical load variation on soil-tire interaction and the accompanying changes in motor torque and rotational characteristics were compared and analyzed.

Each test condition was repeated five times to ensure the reliability and repeatability of the measured data, including soil thrust, slip ratio, and motor load-related parameters. The experimental design conditions are summarized in Table 3.

Table 3 Experimental design conditions

Unit	Condition
Vertical Load (kg)	0, 10, 20, 30, 40
Traveling speed (m/s)	0.5
Traveling distance (m)	3
Number of repetitions	5

Measurement Parameters of the Test System

The tire was driven by a motor mounted on the rotational shaft, and measurement parameters listed in Table 4 were collected using encoders installed inside the motors. The data were recorded at a sampling frequency of 100 Hz.

Table 4 Measured parameters obtained from Motor1 and Motor2

Time	RPM	Torque	Speed	Distance
s	rpm	N·m	m/s	m

Motor1 was directly coupled to the wheel axle through a reducer and served as the driving motor responsible for rotating the tire. In contrast, Motor2, mounted on the pulley, was not involved in driving the tire. Instead, it rotated passively as the tire rotated and measured the actual traveling distance and speed of the tire using its encoder. Therefore, Motor2 did not influence tire driving and was used purely as a sensor for measurement purposes.

Tire Slip

The slip ratio of the tire was calculated using the difference between the theoretical traveling distance generated by tire rotation and the actual traveling distance on the ground. Encoder data measured from Motor1 and Motor2 were used to calculate the slip ratio. The theoretical traveling distance was calculated from the rotational displacement measured by Motor1, and the actual traveling distance was calculated from the rotational displacement measured by Motor2. Based on these values, the slip ratio was defined as shwon in Eq. 3:

$$S = \frac{D_1 - D_2}{D_1} \times 100\ (\%) \qquad (3)$$

Where S: Slip ratio, D_1: Theoretical traveling distance, D_2: Actual travel distance.

In this study, the slip ratio was used as an indicator to quantitatively represent the degree of slippage caused by soil-tire interaction.

Soil Thrust

Soil thrust was defined as the force generated in the driving direction by the tire through interaction with the soil. In this study, soil thrust was calculated using the driving torque measured at Motor1.

The driving torque measured at Motor1 represents the wheel torque acting on the tire rotation axis. By dividing this torque by the tire radius (0.3262 m), soil thrust was defined as shown in Eq. 4:

$$\mathrm{H} = \frac{T_w}{r} \qquad (4)$$

Where H: Soil thrust, T_w: Torque of wheel, r: Tire radius.

Slip Efficiency

In this study, slip efficiency (η_s) was calculated to evaluate the effective traveling performance relative to the driving power input to the tire. Slip efficiency represents the loss associated with the reduction in traveling speed caused by tire slip (Li & Wang, 2014; Stefanow, 2025; Wong, 2024).

In previous studies, tractive efficiency has generally been defined as the ratio of effective tractive power based on net traction force to the input driving power, representing an overall energy efficiency index that includes not only slip losses but also rolling resistance and soil resistance. In contrast, the present study defined slip efficiency based solely on the reduction in actual traveling speed induced by slip.

329 The slip ratio (S) of the tire was defined using the difference between the theoretical traveling
330 speed (V_w) and the actual traveling speed (V_a), as expressed in Eq. 5:

331 $$S = \frac{V_w - V_a}{V_w} \times 100\ (\%) \qquad (5)$$

332 Where S: Slip ratio, V_w: Theoretical driving speed, V_a: Actual driving speed.

333

334 By rearranging Eq. 5 with respect to the actual traveling speed, V_a can be expressed as $V_a =$
335 $(1 - S)V_w$. The effective power generated by the soil thrust (H) at the actual traveling speed
336 was defined as P_{soil}, as shown in Eq. 6 (Zoz & Grisso, 2003):

337 $$P_{soil} = H \times V_a \qquad (6)$$

338 Where P_{soil}: Effective power, H: Soil thrust, V_a: Actual driving speed.

339

340 The input driving power applied to the wheel, P_{wheel}, was defined as the product of wheel
341 torque (T_w) and angular velocity (ω_w), as expressed in Eq. 7 (Zoz & Grisso, 2003):

342 $$P_{wheel} = T_w \times \omega_w \qquad (7)$$

343 Where $\mathrm{P_{wheel}}$: Input power, $\mathrm{T_w}$: Torque of wheel, ω_w: Wheel angular velocity.

344

345 Using the relationship between the wheel angular velocity and the theoretical traveling speed,
346 as given in Eq. 8, together with the definition of soil thrust in Eq. 9, the input driving power
347 can be rewritten as Eq. 10:

348 $$V_w = r \times \omega_w \qquad (8)$$

349 Where V_w: Theoretical driving speed, r: Radius of tire, ω_w: Wheel angular velocity.

350

$$H = \frac{T_w}{r} \qquad (9)$$

Where H: Soil thrust, T_w: Torque of wheel, r: Radius of tire.

$$P_{wheel} = H \times V_w \qquad (10)$$

Where P_{wheel}: Input power, H: Soil thrust, V_w: Theoretical driving speed.

Accordingly, under the condition of identical soil thrust, the ratio of the power effectively used for actual traveling to the input driving power can be expressed as the ratio of the actual traveling speed to the theoretical traveling speed, as shown in Eq. 11 (Stefanow, 2025):

$$\eta_s = \frac{P_{soil}}{P_{wheel}} = \frac{H \times V_a}{H \times V_w} = \frac{V_a}{V_w} = 1 - S \qquad (11)$$

Where η_s: Slip efficiency, P_{soil}: Effective power, P_{wheel}: Input power, V_a: Actual driving speed, V_w: theoretical driving speed, S: Slip ratio.

Based on the above relationships, slip efficiency (η_s) was calculated for each test condition using the measured slip ratio, and the slip behavior and traveling performance characteristics according to variations in vertical load were analyzed.

Gross Traction Coefficient

In this study, the gross traction coefficient was calculated to compare the absolute magnitude of soil thrust under different vertical load conditions and to enable normalized comparison of propulsion performance when vertical loads differed (Zoz & Grisso, 2003). The gross traction coefficient is defined as a dimensionless index obtained by normalizing the soil thrust

generated at the soil-tire contact interface by the vertical dynamic load. This coefficient was used to analyze the relationship between slip and propulsion performance by allowing consistent comparison across varying vertical load conditions (Shafaei et al., 2021). The gross traction coefficient was defined as shown in Eq. 12:

$$\eta_{gt} = \frac{H}{W_{dyn}} \qquad (12)$$

Where μ_{gt}: Gross traction coefficient, H: Soil thrust, W_{dyn}: Vertical dynamic load.

The vertical dynamic load was calculated as the product of gravitational acceleration and the sum of the mass of the drive unit and the additional vertical load, as expressed in Eq. 13:

$$W_{dyn} = (m_{drive} + m_{vertical})g \quad (13)$$

Where W_{dyn}: Vertical dynamic load, m_{drive}: Mass of the drive unit, $m_{vertical}$: Additional vertical load.

All tests were conducted under constant straight-line traveling speed conditions, and the effects of load transfer or inertial forces were not considered. The gross traction coefficient calculated in this study does not represent a traction coefficient based on rolling resistance or drawbar pull, but rather an index based on the total thrust provided by the soil to the tire, namely soil thrust.

The gross traction coefficient used in this study should be interpreted as a supplementary performance index rather than a drawbar-based traction coefficient. In soil-bin experiments where rolling resistance and drawbar pull cannot be independently measured, traction-related indices normalized by vertical load have been widely used to enable relative comparison of soil thrust mobilization under different loading conditions (Zeng et al., 2022; Zoz & Grisso,

2003).

Moreover, previous studies have reported that normalized traction indices do not necessarily vary in the same manner as slip-related efficiency metrics, particularly under deformable soil conditions, highlighting the importance of interpreting gross traction coefficient in conjunction with slip ratio and efficiency rather than as an absolute indicator of tractive performance (Shafaei et al., 2021).

Therefore, this coefficient was used as a supplementary performance indicator to analyze soil shear behavior and thrust mobilization characteristics with respect to variations in slip ratio.

Experimental Soil-bin Tests

Statistical analyses were conducted to quantitatively verify the effects of variations in vertical load on tractive performance. The dependent variables analyzed were Motor1 torque, soil thrust, slip ratio, and slip efficiency. The independent variable was defined as the vertical load condition, and each load level was treated as an independent group.

All experimental data were obtained from five repeated measurements for each vertical load condition. Based on the repeated measurements, descriptive statistics centered on the mean were calculated to examine the basic distributional characteristics of the data. Subsequently, one-way analysis of variance (ANOVA) was applied to determine whether significant differences existed among the mean values across different vertical load conditions (Montgomery, 2013).

Prior to performing ANOVA, the assumption of homogeneity of variances among groups

was assessed using Levene's test. Levene's test evaluates the equality of variances based on the absolute deviations between individual observations and the central tendency of each group. In this study, considering the limited sample size and the potential non-normality of the data distribution, the Levene test statistic based on the median was employed as the measure of central tendency (Brown & Forsythe, 1974; Montgomery, 2013). This approach provides a more robust assessment of variance homogeneity in the presence of non-normal distributions or potential outliers.

When the one-way ANOVA indicated statistically significant differences among vertical load conditions, post hoc analyses were conducted to identify the specific load intervals exhibiting significant differences. To control for the accumulation of Type I error due to multiple comparisons, Tukey's Honestly Significant Difference (HSD) test was applied, following confirmation of variance homogeneity based on the Levene test results. Tukey's HSD compares all possible pairwise group means using a common criterion and is widely used in conjunction with ANOVA to evaluate statistical significance among group means.

In addition, to quantitatively assess the magnitude of the effect of vertical load conditions on each dependent variable, an effect size measure based on ANOVA was calculated. Eta-squared (η^2) was used as the effect size index, enabling evaluation of the relative influence of vertical load variation on each performance indicator.

All statistical analyses were performed using IBM SPSS Statistics (Version 29.0.2.0, IBM Corp., Armonk, NY, USA), and the significance level was set at 0.05.

Results and Discussion

Results of Soil Property Measurements

Based on the particle size distribution analysis conducted to classify the soil used in the soil-bin, the soil was identified as sandy soil. The detailed results are presented in Table 5.

Table 5 Particle size distribution of the soil

Component	Percentage (%)
Sand	96
Silt	2
Clay	2
Soil texture	Sand

The physical and mechanical properties of the soil sampled from the soil-bin are summarized in Table 6. All measured values were calculated as the average of experimental results obtained from samples collected at 16 grid locations.

Table 6 Particle size distribution of the soil

Unit	Value
Bulk density (kg/m^3)	1565.02
Water Content (%)	0.043
Cohesion (kPa)	2.94

Internal friction angle (°)	18.8

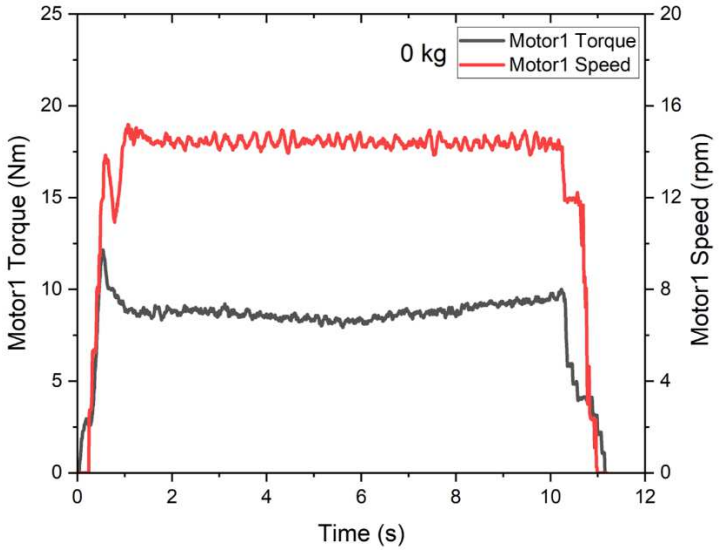
The soil used in this study was dry sandy soil with a particle diameter of 0.18-0.20 mm. The measured water content was approximately 0.04%, indicating that the soil contained negligible moisture. The results of the direct shear test showed that the cohesion was 2.94 kPa and the internal friction angle was 18.8°. According to Eq. 14, due to the inherent characteristics of sandy soil, the cohesion is relatively small, and therefore the shear resistance is predominantly governed by the normal load and the internal friction angle.

$$\tau = c + p \tan \emptyset \qquad (14)$$

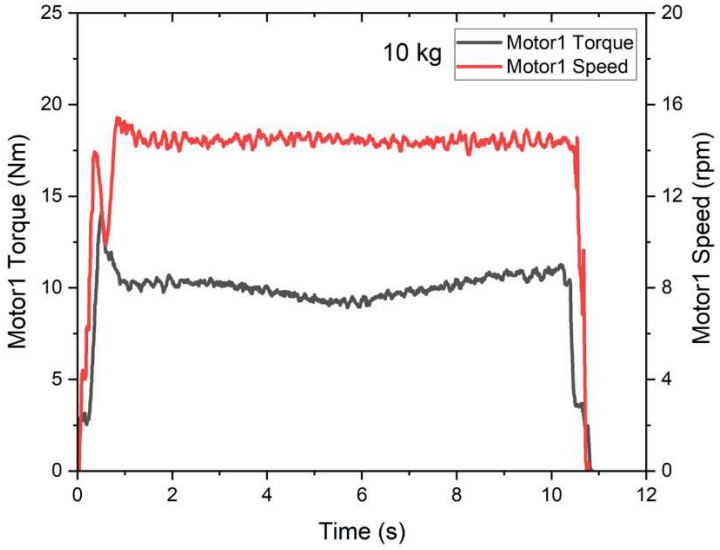
Where τ: Shear stress, c: Cohesion, p: Normal stress, $\emptyset$: Internal friction angle.

Motor Load Analysis Results

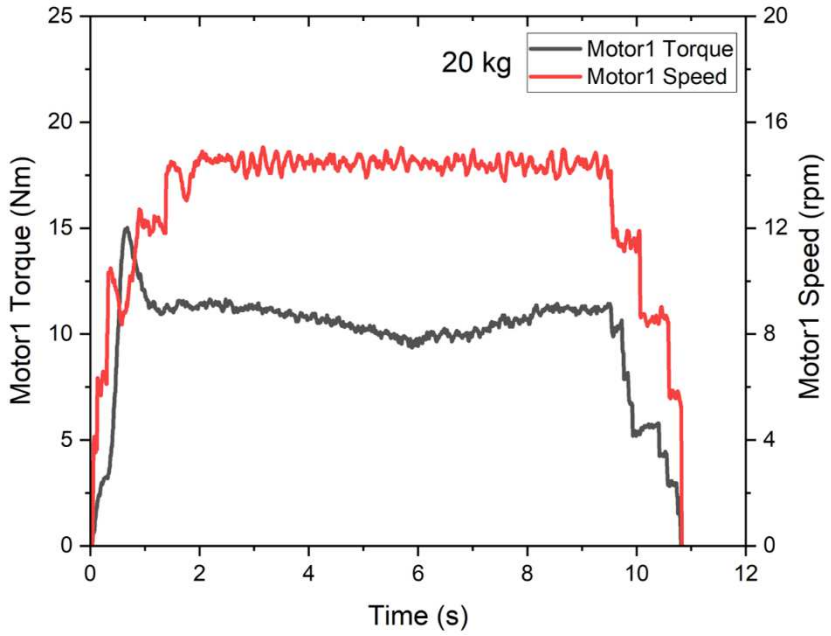
The motor load data analyzed in this study consist of the variations in torque and rotational speed of Motor1 under different normal load conditions. For each normal load condition, the experiment was repeated five times, and the measured data were averaged for analysis. The motor load characteristics according to the normal load conditions are shown in Fig. 8, and the average Motor1 torque values are summarized in Table 7.


0 kg
Motor1 Torque
Motor1 Speed
Motor1 Torque (Nm)
Motor1 Speed (rpm)
Time (s)
0
5
10
15
20
25
0
4
8
12
16
20
0
2
4
6
8
10
12

(a)

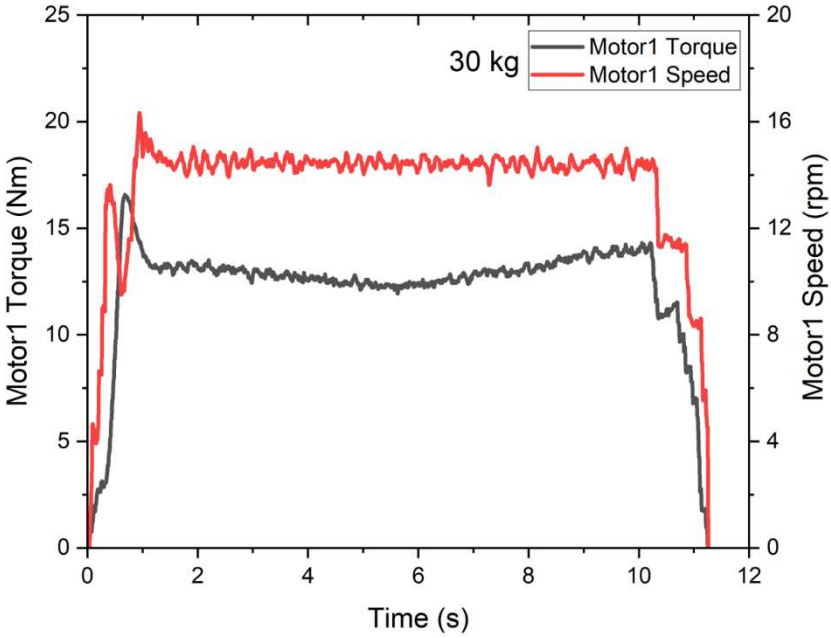

10 kg
Motor1 Torque
Motor1 Speed
Motor1 Torque (Nm)
Motor1 Speed (rpm)
Time (s)
0
5
10
15
20
25
0
4
8
12
16
20
0
2
4
6
8
10
12

(b)



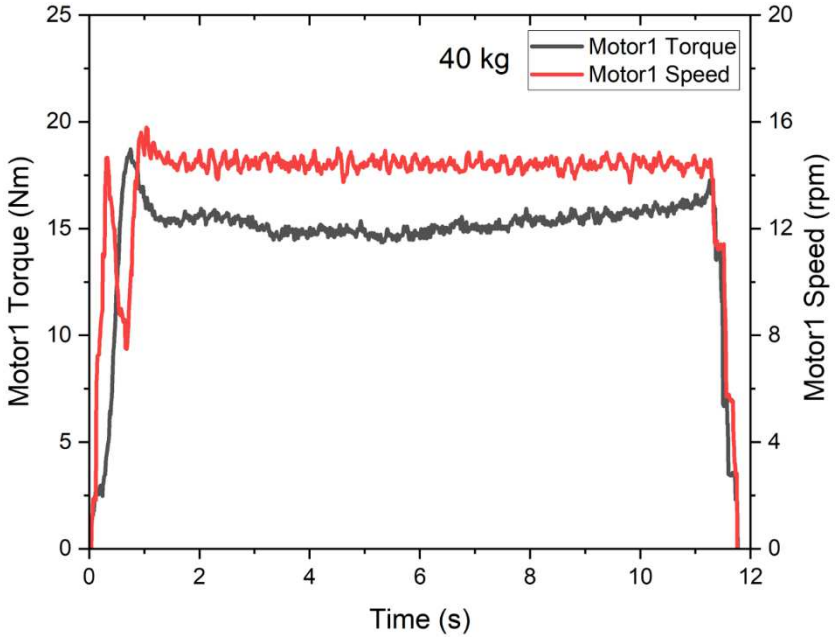
471

472 (c)



473

474 (d)



(e)

Fig.8 Motor load characteristics under different normal load conditions: (a) 0 kg, (b) 10 kg, (c) 20 kg, (d) 30 kg, (e) 40 kg.

Table 7 Average motor torque and speed under different normal load conditions

Normal Load	Motor1 Torque	Motor1 Speed
kg	N·m	rpm
0	8.824	
10	10.052	
20	10.703	14.6
30	13.001	
40	15.317	

The average motor torque was lowest under the 0 kg normal load condition, with a value of approximately 8.82 N·m. Under the 40 kg condition, the average motor torque increased to approximately 15.32 N·m, representing an increase of about 1.74 times compared to the 0 kg condition. Because the traveling speed was maintained at 0.5 m/s during the test design, the motor rotational speed in the working section remained nearly constant at an average value of approximately 14.6 rpm for all normal load conditions. This result indicates that the drive control system of the test apparatus was able to stably maintain the motor rotational speed despite variations in the applied normal load.

As the normal load increased, the average motor torque in the working section exhibited an overall increasing trend. The results of the one-way analysis of variance (ANOVA) conducted to examine the differences in mean motor torque among the normal load conditions are presented in Table 8, and the results of Levene's test are shown in Table 9.

Table 8 Results of one-way ANOVA for Motor1 torque

ANOVA		ANOVA effect size
Between-group		
F	p-value	η^2
222.417	< 0.001	0.978

Table 9 Results of Levene′s test for Motor1 torque

Median based

Levene's statistic	df1	df2	p-value
1.479	4	20	0.246

The one-way ANOVA results indicated that the main effect of the normal load condition was statistically significant ($F = 222.417$, $p < 0.001$). The effect size obtained from the ANOVA was $\eta^2 = 0.978$, indicating that the normal load condition had a strong influence on the variation in motor torque. This result confirms that an increase in normal load is a major factor that significantly increases the torque demand of the motor.

The Levene's test conducted to evaluate the homogeneity of variances showed a median-based significance value of 0.246 ($p > 0.05$), satisfying the assumption of equal variances. Accordingly, Tukey's honestly significant difference (HSD) post-hoc test was applied, and the results are presented in Table 10.

Table 10 Results of Tukey′s HSD post-hoc test for Motor1 torque

Comparison	Mean difference	p-value	Separation
0-10 kg	-1.301	< 0.01	separated
10-20 kg	-0.677	0.080	borderline
20-30 kg	-2.267	< 0.01	separated
30-40 kg	-2.288	< 0.01	separated

The post-hoc analysis revealed that the average motor torque increased significantly in the 0-10 kg, 20-30 kg, and 30-40 kg intervals ($p < 0.001$). In contrast, although an increase in

514 average motor torque was observed between the 10-20 kg conditions, the difference between
515 these two conditions was classified as borderline at the 0.05 significance level ($p = 0.080$). This
516 result suggests that, in the low normal load range, the motor torque response to increasing load
517 is relatively gradual, whereas a more pronounced increase in torque demand occurs beyond a
518 certain load threshold.

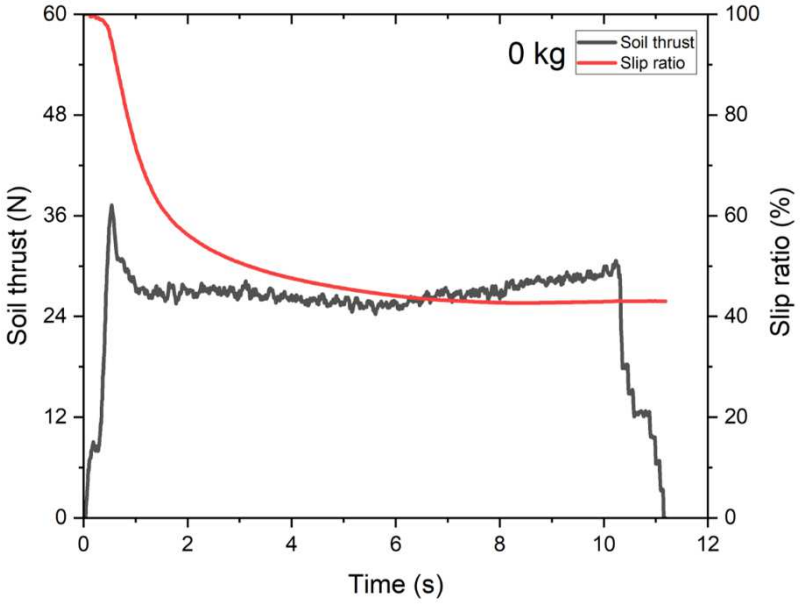
519 The changes in motor load characteristics according to the normal load conditions are further
520 discussed in the following section in relation to variations in soil thrust, slip behavior, and slip
521 efficiency.

522

523 ## Tractive Performance Analysis Results

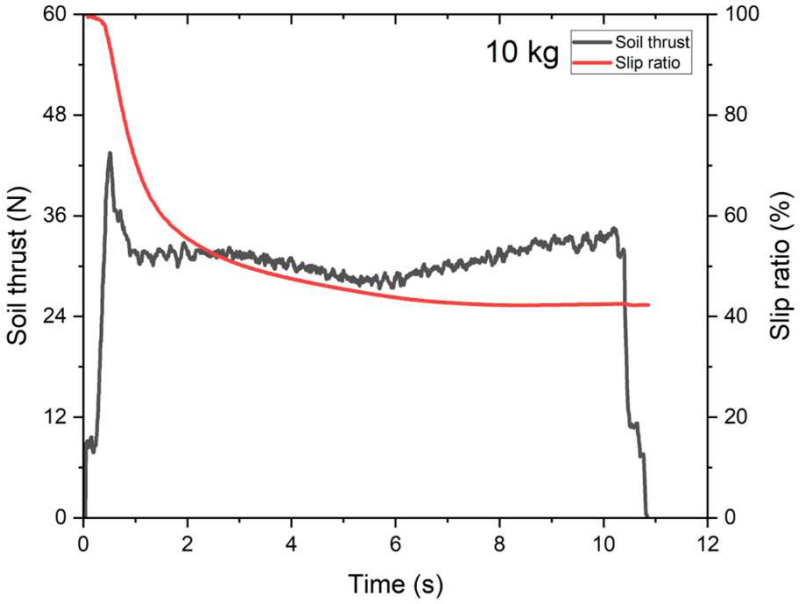
524 The tractive performance parameters evaluated in this study were the slip ratio (S), soil thrust
525 (H), slip efficiency (η_S), and gross traction coefficient (μ_{gt}). For each normal load condition,
526 the experiments were repeated five times, and the results were summarized using the mean
527 values. The slip ratio and soil thrust measured under different normal load conditions are
528 presented in Fig. 9. In addition, the average and maximum values of soil thrust, the average
529 slip ratio, the average slip efficiency, and the average gross traction coefficient are summarized
530 in Table 11.

531



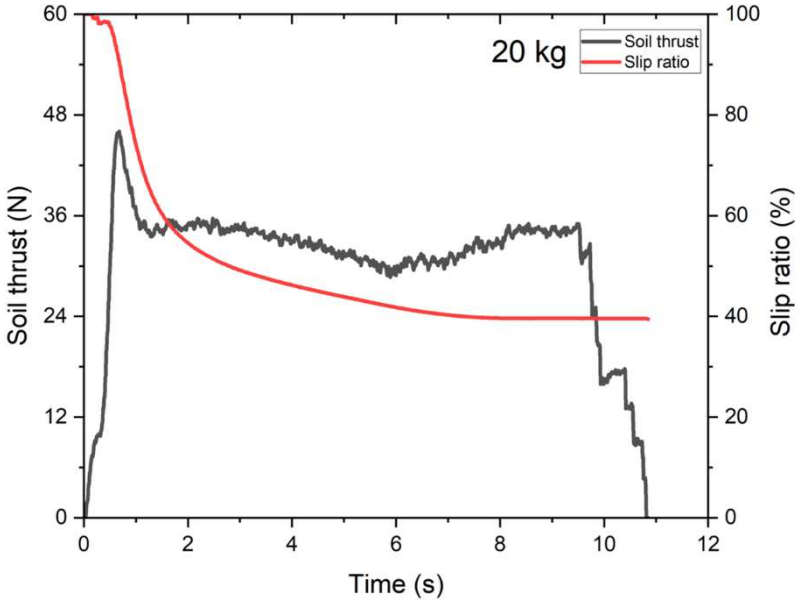
532

533 (a)



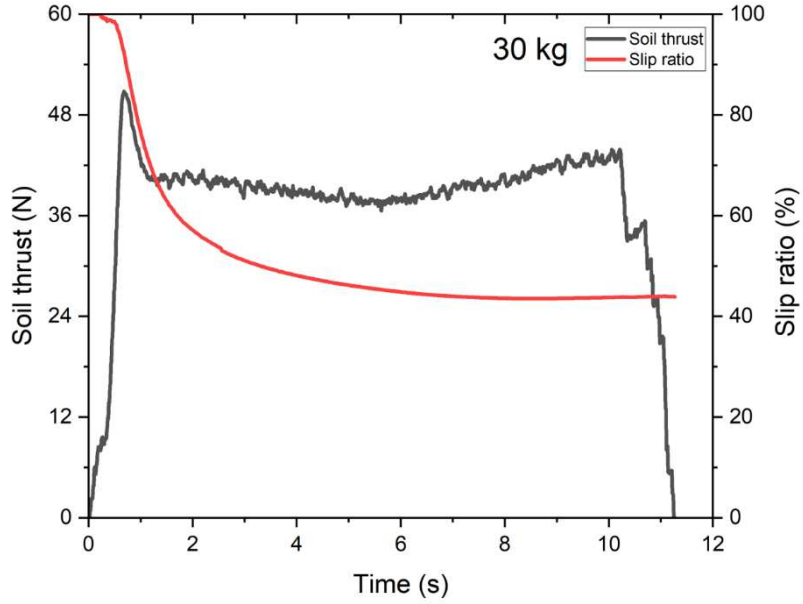
534

535 (b)



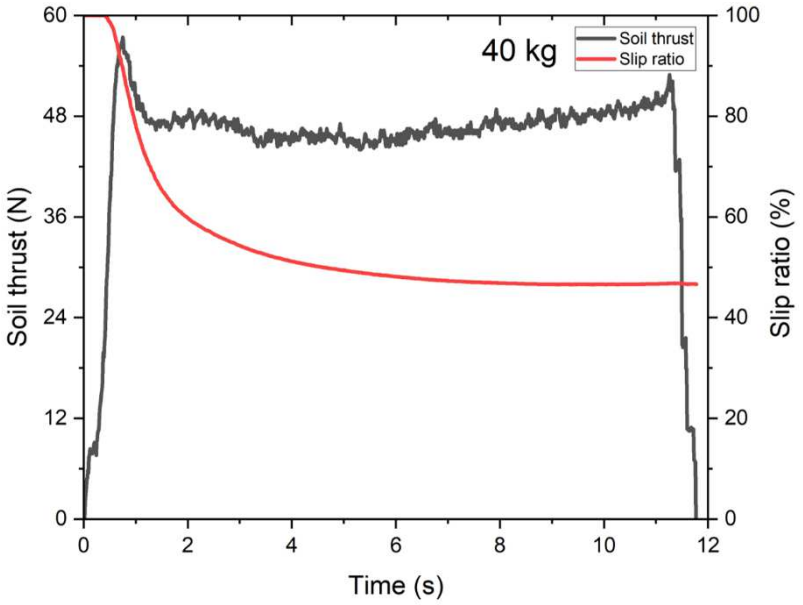
536

537 (c)



538

539 (d)



(e)

Fig.9 Soil thrust and slip ratio under different normal load conditions: (a) 0 kg, (b) 10 kg, (c) 20 kg, (d) 30 kg, (e) 40 kg.

Table 11 Average and maximum of soil thrust, average of slip ratio, slip efficiency and gross traction coefficient

Normal Load	H		S	η_s	μ_{gt}
	Average	Max	Average		
kg	N		%		-
0	27.073	37.279	49.346	50.654	0.0438
10	31.013	43.508	48.636	51.364	0.0433
20	33.144	46.071	46.901	53.099	0.0407
30	40.085	50.829	49.551	50.449	0.0439
40	47.194	57.426	52.064	47.939	0.0467

548 The results of the one-way analysis of variance (ANOVA) conducted to examine the
549 statistical significance of the mean differences in tractive performance parameters according to
550 the normal load conditions are presented in Table 12, and the results of Levene's homogeneity
551 of variance test are shown in Table 13.

552

553 **Table 12** Results of one-way ANOVA for tractive performance parameters

	ANOVA		ANOVA effect size
	Between-group		
	F	p-value	η^2
H	222.417	< 0.001	0.978
S	6.738	0.001	0.489
η_S	6.739	0.001	0.574

554

555 **Table 13** Results of Levene′s test for tractive performance parameters

	Median based			
	Levene's statistic	df1	df2	p-value
H	19.243	4	20	0.246
S	3.106	4	20	0.279
η_S	3.105	4	20	0.273

556

557 The one-way ANOVA results indicated that the mean differences among normal load
558 conditions were statistically significant for all three parameters. For soil thrust, a very high

559 level of statistical significance was observed ($F = 222.417$, $p < 0.001$), with an effect size of
560 0.978. This result indicates that, under sandy soil conditions, the normal load plays a dominant
561 role in variations of soil thrust and the formation of tractive force.

562 The mean differences in slip ratio and slip efficiency were also statistically significant, with
563 effect sizes of 0.489 and 0.574, respectively, indicating that the normal load condition
564 significantly influenced both parameters.

565 Based on the median-centered Levene's test results, the significance levels for all three
566 parameters exceeded 0.05, confirming that the assumption of homogeneity of variances was
567 satisfied. Therefore, the ANOVA results obtained in this study can be interpreted under the
568 assumption of equal variances, and Tukey's HSD post-hoc test was subsequently applied. The
569 post-hoc test results are summarized in Table 14.

570

571 **Table 11** Results of Tukey′s HSD post-hoc test for Motor1 torque

	Comparison		Mean difference	p-value	Separation
Soil thrust	0-10 kg		-1.301	< 0.001	separated
	10-20 kg		-0.677	0.080	borderline
	20-30 kg		-2.267	< 0.001	separated
	30-40 kg		-2.288	< 0.001	separated
Slip ratio & Slip Efficiency	0 kg	10 kg	0.811	0.881	not separated
		20 kg	2.270	0.107	not separated
		30 kg	0.085	1.000	not separated
		40 kg	-2.145	0.139	not separated

		20 kg	1.458	0.470	not separated
	10 kg	30 kg	-0.727	0.917	not separated
		40 kg	-2.956	0.021	separated
	20 kg	30 kg	-2.185	0.128	not separated
		40 kg	-4.414	0.001	not separated
	30 kg	40 kg	2.229	0.001	separated

572

573 As the normal load increased, the average soil thrust exhibited an approximately linear
574 increasing trend. The average soil thrust increased from approximately 27.07 N at the 0 kg
575 condition to approximately 47.19 N at the 40 kg condition, representing an increase of about
576 1.74 times. The maximum soil thrust showed a trend similar to that of the average values,
577 confirming that increasing normal load played a dominant role in soil thrust generation. This
578 behavior can be attributed to the expansion of the soil-tire contact area and the concurrent
579 increase in soil bearing capacity and shear resistance with increasing normal load.

580 According to the results of Tukey's HSD post-hoc test, the average soil thrust increased
581 significantly in the 0-10 kg, 20-30 kg, and 30-40 kg intervals ($p < 0.001$). In contrast, although
582 an increase in average soil thrust was observed between the 10 kg and 20 kg conditions, the
583 difference was classified as borderline at the 0.05 significance level ($p = 0.080$). This result
584 suggests that, in the low-load region, soil shear resistance is gradually mobilized with
585 increasing load, resulting in a relatively moderate increase in soil thrust.

586 Meanwhile, the increase in soil thrust with increasing normal load should be interpreted not
587 only as a change in tractive performance at the soil-tire interface, but also in conjunction with
588 the increased load demand imposed on the tire drive system. As the normal load increases, tire

589 sinkage and contact area increase, leading to higher soil deformation resistance and rolling
590 resistance, which in turn increase the torque required to drive the tire. Therefore, the observed
591 increase in soil thrust under identical traveling speed conditions does not necessarily indicate
592 an improvement in pure tractive efficiency, but rather reflects the combined effect of increased
593 input load to the drive system.

594 The slip ratio behavior with respect to changes in normal load did not exhibit a monotonic
595 increasing or decreasing trend, but instead showed non-monotonic behavior, with minimum or
596 maximum values occurring at specific load conditions. This trend differs from the
597 approximately linear increase observed in Motor1 torque and soil thrust with increasing normal
598 load.

599 At the 0 kg and 10 kg normal load conditions, the average slip ratios were approximately
600 49.35% and 48.64%, respectively, which are relatively high values. This indicates that, in the
601 low-load region, insufficient effective soil shear resistance was mobilized, causing the tire to
602 experience rolling accompanied by substantial slip. In contrast, at the 20 kg condition, the
603 average slip ratio reached its minimum value of approximately 46.90%, suggesting that the soil
604 was compacted to an appropriate degree and that shear strength was effectively mobilized at
605 the soil-tire interface (Damanauskas & Janulevičius, 2015; Koolen & Kuipers, 1983; Md-Tahir
606 et al., 2019; Rasool & Raheman, 2018). This indicates that the balance between soil shear
607 resistance and soil compaction was most stable at this load condition.

608 As the normal load further increased to 30 kg and 40 kg, the average soil thrust continued to
609 increase; however, the average slip ratio increased again to approximately 49.55% and 52.06%,
610 respectively. According to the Tukey's HSD post-hoc test results, the differences in average
611 slip ratio between the 20-30 kg and 30-40 kg conditions ($p = 0.128$ and $p = 0.116$) were not

statistically significant at the 0.05 level. However, the 40 kg condition exhibited a significantly higher average slip ratio compared to the 10 kg and 20 kg conditions ($p = 0.021$ and $p < 0.001$). This behavior can be interpreted as the result of excessive tire sinkage and localized shear deformation and shear failure in the surrounding soil under high-load conditions (30 and 40 kg). Consequently, although soil thrust increased, the accompanying increase in soil resistance led to a higher slip ratio.

The average graph of slip efficiency according to normal load is shown in Fig. 10.

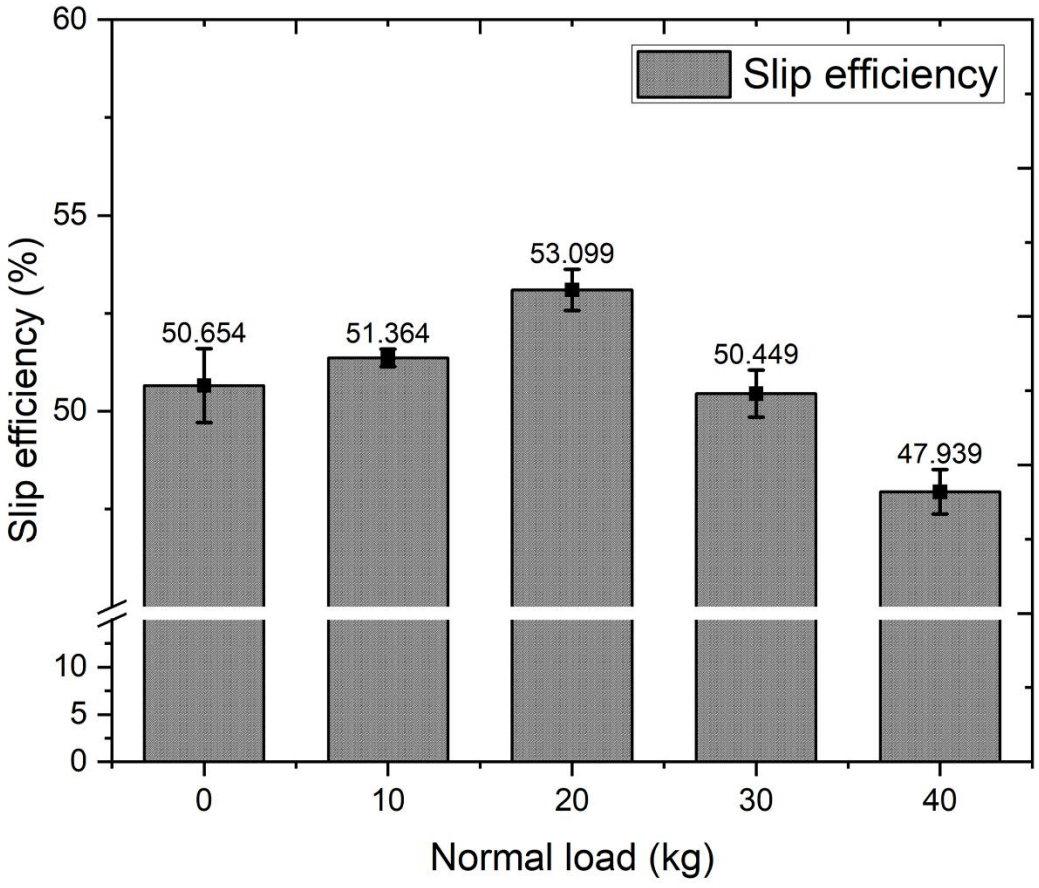


Fig.10 Slip efficiency under different normal load conditions.

Slip efficiency also exhibited non-monotonic behavior similar to that of the slip ratio, which can be interpreted as the result of the interaction between increasing drive load and slip behavior with increasing normal load. As the required load on the tire drive system increases, the extent to which the input driving energy is effectively converted into actual tractive performance is governed by slip behavior. Slip acts as a loss mechanism, whereby input energy is dissipated through soil deformation and relative motion. Beyond a certain normal load level, additional input load may not be converted into increased soil thrust, but instead leads to increased slip. Under such conditions, the rate of increase in effective tractive performance relative to the input load decreases, resulting in a reduction in slip efficiency.

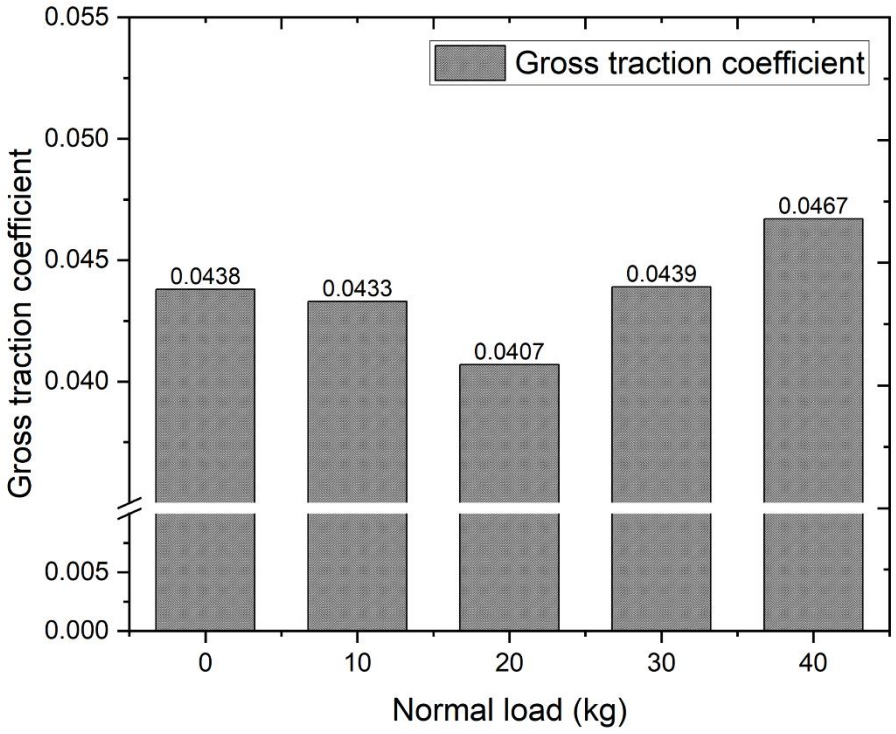
The average slip efficiency reached its maximum value of approximately 53.1% at the 20 kg normal load condition, which coincided with the condition exhibiting the minimum slip ratio. In contrast, the lowest average slip efficiency of approximately 47.94% was observed at the 40 kg condition.

According to the Tukey's HSD post-hoc test results, the differences in average slip efficiency between the 20-30 kg and 30-40 kg conditions were not statistically significant ($p = 0.128$ and $p = 0.116$). However, the 40 kg condition showed a statistically significant decrease in average slip efficiency compared to the 10 kg and 20 kg conditions ($p = 0.021$ and $p < 0.001$). These results indicate that even when the absolute magnitude of soil thrust increases, slip efficiency can decrease if the increase is accompanied by a higher slip ratio. Under the present test conditions, a normal load of approximately 20 kg provided the most balanced condition for mobilizing soil shear resistance while suppressing excessive slip. Thus, slip ratio and slip efficiency do not exhibit a simple monotonic relationship with increasing normal load, but rather demonstrate non-monotonic characteristics.

646 To normalize and compare the level of mobilized soil shear resistance under different normal
647 load conditions, the gross traction coefficient was calculated. This dimensionless parameter,
648 defined as the ratio of soil thrust to the vertical dynamic load, enables relative comparison of
649 tractive performance even under different load conditions. The average gross traction
650 coefficient at the 0 kg condition was approximately 0.0438, which was similar to that at the 10
651 kg condition. At the 20 kg condition, the value decreased to 0.0407, but increased to a
652 maximum of 0.0467 as the normal load increased to 30 kg and 40 kg.

653 The average gross traction coefficient as a function of normal load is shown in Fig. 11.

654



655

656 **Fig.11** Gross traction coefficient under different normal load conditions.

657

658 The calculated gross traction coefficient ranged from approximately 0.04 to 0.05,

corresponding to about 6-12% of the gross traction coefficient range (0.39-0.81) reported for tractors equipped with lug tires under tillage conditions (Shafaei et al., 2021). The gross traction coefficient is a dimensionless parameter obtained by normalizing soil thrust by the vertical dynamic load, and its absolute magnitude varies substantially depending on tire geometry and soil conditions (Wong, 2024; Zoz & Grisso, 2003). In particular, under dry sandy soil conditions with negligible moisture content, the mobilization of shear resistance at the soil-tire interface is limited, resulting in relatively low soil thrust. Previous soil-bin studies on granular soils have also reported that traction force and traction coefficient levels are strongly influenced by ground properties (Zeng et al., 2022). Due to these condition-specific differences, the gross traction coefficient obtained in this study appeared at a low level.

As shown in Table 11 and Fig. 11, although the average soil thrust increased continuously with increasing normal load, the gross traction coefficient exhibited non-monotonic behavior, reaching a minimum value (0.0407) at 20 kg and increasing again in the 30-40 kg range. This indicates that, under conditions where both soil thrust and vertical dynamic load increase simultaneously, the rate of increase in soil thrust does not remain proportional to the rate of increase in normal load (Shafaei et al., 2021). Meanwhile, the fact that the gross traction coefficient reached its minimum value at 20 kg does not directly align with the results showing the minimum slip ratio (46.901%) and maximum slip efficiency (53.099%) at the same load condition. This discrepancy arises because the gross traction coefficient represents the normalized level of mobilized soil thrust, whereas slip ratio and slip efficiency more directly reflect losses associated with the conversion of input load into actual traveling motion. Therefore, even when the gross traction coefficient increases under the 30-40 kg conditions, an accompanying increase in slip ratio and decrease in slip efficiency may still occur. The present results demonstrate that the mobilization level of soil thrust (gross traction coefficient) and slip

efficiency do not necessarily vary in the same direction.

As the normal load increased from 0 kg to 40 kg under sandy soil conditions, the average soil thrust increased from approximately 27.07 N to 47.19 N, corresponding to a 1.74-fold increase. Under the same conditions, the average slip ratio decreased to a minimum of approximately 46.90% at 20 kg and then increased to approximately 52.06% at 40 kg, while the average slip efficiency decreased from approximately 53.1% to 47.94%. These results quantitatively demonstrate that although increasing normal load contributes to an increase in the absolute magnitude of soil thrust, excessive sinkage and localized shear failure at higher load levels can lead to increased slip and a reduction in tractive efficiency. Therefore, to achieve optimal tractive performance, it is necessary to determine an appropriate normal load condition by considering not only the magnitude of soil thrust, but also slip ratio and slip efficiency simultaneously.

Conclusions

In this study, the effects of variations in normal load on the tractive performance of a single tire under sandy soil conditions were experimentally investigated using a soil-bin. Repeated straight-line traveling tests were conducted while incrementally increasing the normal load, and soil thrust, slip ratio, slip efficiency, and gross traction coefficient were quantitatively evaluated.

The experimental results showed that soil thrust generally increased with increasing normal load, and the average soil thrust at the 40 kg condition increased by approximately 1.74 times compared to that at the 0 kg condition. This result indicates that, under sandy soil conditions,

normal load plays a dominant role in the formation of soil thrust. In contrast, slip ratio and slip efficiency did not exhibit monotonic trends with increasing normal load. Instead, non-monotonic behavior was observed, with the minimum slip ratio and maximum slip efficiency occurring at approximately the 20 kg condition. Meanwhile, the gross traction coefficient also exhibited non-monotonic behavior with respect to normal load, suggesting that it can be used as a supplementary indicator for comparing the normalized level of mobilized soil thrust under different load conditions.

These results indicate that variations in normal load do not lead to monotonic changes in tractive performance under sandy soil conditions. While increasing normal load consistently enhanced the absolute magnitude of soil thrust, slip-related performance indicators exhibited non-monotonic behavior, demonstrating the existence of an optimal normal load condition that cannot be identified based on thrust magnitude alone. This finding highlights the importance of jointly evaluating soil thrust and slip-related efficiency metrics when assessing load-dependent tractive performance.

As the normal load increased, the load demand on the drive system increased accordingly. However, under high normal load conditions, an increase in slip ratio was accompanied by a decrease in slip efficiency. This indicates that even when the absolute magnitude of soil thrust increases, the efficiency of conversion into effective tractive performance can decrease if slip losses increase simultaneously. Therefore, to achieve optimal tractive performance under sandy soil conditions, it is necessary to determine an appropriate normal load condition by jointly considering soil thrust, slip ratio, and slip efficiency, rather than relying solely on the magnitude of thrust.

The present study was conducted under indoor soil-bin test conditions using a single tire,

and individual soil reaction components such as tire sinkage, rolling resistance, and bulldozing resistance were not separately measured. In future studies, simultaneous measurement of tire sinkage and independent evaluation of soil resistance components will be required to more quantitatively elucidate the soil-tire interaction mechanisms associated with increasing normal load. The soil-bin-based experimental results obtained in this study are expected to be useful as validation data for DEM-MBD coupled simulations or soil-tire interaction models. In addition, the tractive performance data acquired through the soil-bin can serve as experimental benchmark data for the validation and advancement of traction performance prediction models for off-road machinery, including agricultural machinery, construction equipment, and robotic platforms.

Conflict of Interest

The authors have no conflicting financial or other interests.

Funding This work was supported by the Korea Institute of Planning and Evaluation for Technology in Food, Agriculture and Forestry (IPET) through the Agri-Food Export Enhancement Technology Development Program, funded by the Ministry of Agriculture, Food and Rural Affairs (MAFRA) (RS-2023-00233191), and by the ″Busan Regional Innovation System & Education (RISE)″ Project, supported by the Ministry of Education and Busan Metropolitan City.

Declarations

Ethical Approval Not applicable.

Competing interests The authors declare no competing interests.

References

Alkhalifa, N., Tekeste, M. Z., Jjagwe, P., & Way, T. R. (2024). Effects of vertical load and inflation pressure on tire-soil interaction on artificial soil. Journal of Terramechanics, 112, 19–34. https://doi.org/10.1016/j.jterra.2023.11.002

Ani, O. A., Uzoejinwa, B. B., Ezeama, A. O., Onwualu, A. P., Ugwu, S. N., & Ohagwu, C. J. (2018). Overview of soil-machine interaction studies in soil bins. Soil and Tillage Research, 175, 13–27. https://doi.org/10.1016/j.still.2017.08.002

Bahrami, M., Naderi-Boldaji, M., Ghanbarian, D., & Keller, T. (2023). Discrete element modelling of stress propagation in soil under a rigid wheel in a soil bin: a simulation of probe inducing stress deviation and wheel speed. Biosystems Engineering, 230(4), 159–170. https://doi.org/10.1016/S1537-5110(03)00069-2

Bailey, A. C., Raper, R. L., Way, T. R., Burt, E. C., & Johnson, C. E. (1996). Soil stresses under a tractor tire at various loads and inflation pressures. Journal of Terramechanics, 33(1), 1–11. https://doi.org/10.1016/0022-4898(96)00004-3

Brown, M. B., & Forsythe, A. B. (1974). Robust Tests for the Equality of Variances. Source: Journal of the American Statistical Association, 69(346), 364–367. https://doi.org/https://doi.org/10.1080/01621459.1974.10482955

Calleja-Huerta, A., Lamandé, M., Green, O., & Munkholm, L. J. (2023). Impacts of load and repeated wheeling from a lightweight autonomous field robot on the physical properties

772 of a loamy sand soil. Soil and Tillage Research, 233(3), 105791.
773 https://doi.org/10.1016/j.still.2023.105791

774 Damanauskas, V., & Janulevičius, A. (2015). Differences in tractor performance parameters
775 between single-wheel 4WD and dual-wheel 2WD driving systems. Journal of
776 Terramechanics, 60, 63–73. https://doi.org/10.1016/j.jterra.2015.06.001

777 Farhadi, P., Golmohammadi, A., Sharifi Malvajerdi, A., & Shahgholi, G. (2020). Tire and soil
778 effects on power loss: Measurement and comparison with finite element model results.
779 Journal of Terramechanics, 92, 13–22. https://doi.org/10.1016/j.jterra.2020.09.004

780 Gee-Clough, D. (1976). The Bekker theory of rolling resistance amended to take account of
781 skid and deep sinkage. Journal of Terramechanics, 13(2), 87–105.
782 https://doi.org/10.1016/0022-4898(76)90016-1

783 Jjagwe, P., Tekeste, M. Z., Alkhalifa, N., & Way, T. R. (2023). Modeling tire-soil compression
784 resistance on artificial soil using the scaling law of pressure-soil sinkage relationship.
785 Journal of Terramechanics, 108, 7–19. https://doi.org/10.1016/j.jterra.2023.02.002

786 Karpman, E., Kövecses, J., Holz, D., & Skonieczny, K. (2020). Discrete element modelling for
787 wheel-soil interaction and the analysis of the effect of gravity. Journal of Terramechanics,
788 91, 139–153. https://doi.org/10.1016/j.jterra.2020.06.002

789 Kawase, Y., Nakashima, H., & Oida, A. (2006). An indoor traction measurement system for
790 agricultural tires. Journal of Terramechanics, 43(3), 317–327.
791 https://doi.org/10.1016/j.jterra.2005.05.007

792 Kim, W. S., Kim, Y. J., Baek, S. M., Baek, S. Y., Moon, S. P., Lee, N. G., Kim, T. J., Siddique,

M. A. A., Jeon, H. H., & Kim, Y. S. (2020). Effect of the Cone Index on the Work Load of the Agricultural Tractor. Journal of Drive and Control, 17(2), 9–18. https://doi.org/10.7839/ksfc.2020.17.2.009

Koolen, A. J., & Kuipers, H. (1983). Agricultural Soil Mechanics (Vol. 13). Springer Berlin Heidelberg. https://doi.org/10.1007/978-3-642-69010-5

Li, Z., & Wang, Y. (2014). Coordinated control of slip ratio for wheeled mobile robots climbing loose sloped terrain. Scientific World Journal, 2014. https://doi.org/10.1155/2014/396382

Mahadi, M. R., Chen, Y., & Botha, P. (2017). Instrumented soil bin for testing soil-engaging tools. Applied Engineering in Agriculture, 33(3), 357–366. https://doi.org/10.13031/aea.11874

Mardani, A., & Golanbari, B. (2024). Indoor measurement and analysis on soil-traction device interaction using a soil bin. Scientific Reports, 14(1). https://doi.org/10.1038/s41598-024-59800-2

Md-Tahir, H., Zhang, J., Xia, J., Zhang, C., Zhou, H., & Zhu, Y. (2019). Rigid lugged wheel for conventional agricultural wheeled tractors – Optimising traction performance and wheel–soil interaction in field operations. Biosystems Engineering, 188(4), 14–23. https://doi.org/10.1016/j.biosystemseng.2019.10.001

Montgomery, D. C. (2013). Design and analysis of experiments. John Wiley & Sons, Inc.

Park, C., & Jeong, J. (2018). Characteristics of Shear Strength Parameters of Various Soils by Direct Shear Test. TUNNEL & UNDERGROUND SPACE, 28(6), 584–595. https://doi.org/10.7474/TUS.2018.28.6.584

814 Ptak, W., Czarnecki, J., Brennensthul, M., Lejman, K., & Małecka, A. (2023). Evaluation of
815 Tires Acting on Soil in Field Conditions Using the 3D Scanning Method. Agriculture
816 (Switzerland), 13(5). https://doi.org/10.3390/agriculture13051094

817 Rasool, S., & Raheman, H. (2018). Improving the tractive performance of walking tractors
818 using rubber tracks. Biosystems Engineering, 167, 51–62.
819 https://doi.org/10.1016/j.biosystemseng.2017.12.013

820 Roozbahani, A., Mardani, A., Jokar, R., & Taghavifar, H. (2013). Evaluating and Measuring
821 the Performance Parameters of Agricultural Wheels. Journal of Agricultural and
822 Biosystems Engineering, 7(2), 158–162.
823 https://doi.org/https://doi.org/10.5281/ZENODO.1326774

824 Shafaei, S. M., Loghavi, M., & Kamgar, S. (2021). Fundamental realization of longitudinal slip
825 efficiency of tractor wheels in a tillage practice. Soil and Tillage Research, 205, 104765.
826 https://doi.org/10.1016/j.still.2020.104765

827 Shmulevich, I., Ronai, D., & Wolf, D. (1996). A new field single wheel tester. Journal of
828 Terramechanics, 33(3), 133–141. https://doi.org/10.1016/S0022-4898(96)00014-6

829 Stefanow, D. (2025). The Impact of Transfer Case Parameters on the Tractive Efficiency of
830 Heavy Off-Road Vehicles. Sustainability, 17(19). https://doi.org/10.3390/su17198586

831 Taghavifar, H., & Mardani, A. (2014). Analyses of energy dissipation of run-off-road wheeled
832 vehicles utilizing controlled soil bin facility environment. Energy, 66, 973–980.
833 https://doi.org/10.1016/j.energy.2014.01.076

834 Taghavifar, H., Mardani, A., & Karim-Maslak, H. (2014). Multi-criteria optimization model to

investigate the energy waste of off-road vehicles utilizing soil bin facility. Energy, 73(1), 762–770. https://doi.org/10.1016/j.energy.2014.06.081

Tan, K. H. (2005). Soil Sampling, Preparation, and Analysis. https://doi.org/https://doi.org/10.1201/9781482274769

Tiwari, V. K., Pandey, K. P., & Pranav, P. K. (2010). A review on traction prediction equations. Journal of Terramechanics, 47(3), 191–199. https://doi.org/10.1016/j.jterra.2009.10.002

Wong, J. Y. (2024). Terramechanics and Off-Road Vehicle Engineering: Terrain Behaviour and Off-Road Mobility. Butterworth-Heinemann.

Yang, P., Zang, M., & Zeng, H. (2020). DEM–FEM simulation of tire–sand interaction based on improved contact model. Computational Particle Mechanics, 7(4), 629–643. https://doi.org/10.1007/s40571-019-00293-6

Zeng, H., Xu, W., & Zang, M. (2022). Experimental investigation of tire traction performance on granular terrain. Journal of Terramechanics, 104, 49–58. https://doi.org/10.1016/j.jterra.2022.09.002

Zhou, L., Gao, J., Hu, C., & Li, Q. (2021). Numerical simulation and testing verification of the interaction between track and sandy ground based on discrete element method. Journal of Terramechanics, 95, 73–88. https://doi.org/10.1016/j.jterra.2021.03.002

Zoz, F. M., & Grisso, R. D. (2003). Traction and Tractor Performance. www.asae.org